Draft version June 17, 2023
Typeset using LaTeX **twocolumn** style in AASTeX631

Roman CCS White Paper: Galactic Bulge Time Domain Survey: Mass measurement of FFP with source color measurements

Takahiro Sumi,[1] Matthew T. Penny,[2] Samson A. Johnson,[3] Naoki koshimoto,[1] Shota Miyazaki,[4] and Daisuke Suzuki[1]

[1] *Department of Earth and Space Science, Graduate School of Science, Osaka University, Toyonaka, Osaka 560-0043, Japan*
[2] *Louisiana State University, 261-B Nicholson Hall, Tower Dr., Baton Rouge, LA 70803-4001, USA*
[3] *Jet Propulsion Laboratory*
[4] *Institute of Space and Astronautical Science, Japan Aerospace Exploration Agency, 3-1-1 Yoshinodai, Chuo, Sagamihara, Kanagawa 252-5210, Japan*

ABSTRACT

We can measure the lens mass from the angular Einstein radius $\theta_{\rm E}$ in combination with the (space) microlensing parallax. The $\theta_{\rm E}$ measurement alone is still useful for constraining the mass of the lens objects even without the microlensing parallax. The $\theta_{\rm E}$ can be estimated from the finite source size effect parameter $\rho = \theta_*/\theta_{\rm E}$ from the light curve. Here the source color is needed to estimate the source angular radius θ_* to derive $\theta_{\rm E}$. A typical timescale of magnification by a terrestrial mass Free-floating planet (FFP) is a few hours. Therefore, it is important to increase the observational cadence with other passbands in the Galactic Bulge Time Domain survey as possible. The color information during the magnification is also useful for discriminating the real microlensing event due to FFP from flare stars which are the major contaminants in the very short timescale events. To measure the mass function of FFP down to an Earth mass. The detection efficiency for short events depends on both $t_{\rm E}$ and $\theta_{\rm E}$, and it is important to measure the color of sources as possible.

Keywords: gravitational microlensing; exoplanet; Free floating planets

1. INTRODUCTION

The planet-planet scattering during the planet formation process is likely to produce a population of free-floating planets (FFP) or wide orbit planetary mass objects (Rasio & Ford 1996; Weidenschilling & Marzari 1996; Lin & Ida 1997). It is important to measure the mass functions (MFs) of FFP to understand the formation mechanism of the exoplanets and FFP. Gravitational microlensing observations is the only method to detect FFP and measure of their MFs (Paczyński 1991; Sumi et al. 2011; Mróz et al. 2017, 2019, 2020a). Sumi et al. (2011); Mróz et al. (2017) interpreted the detection of short timescale microlensing events as evidence for the existence of a population of FFP and/or wide orbit planets.

These studies are based on distribution of Einstein radius crossing time $t_{\rm E}$, which is proportional to the square root of the lens mass M as follows,

$$\begin{aligned} t_{\rm E} &= \frac{\sqrt{\kappa M \pi_{\rm rel}}}{\mu_{\rm rel}} \\ &= 1\,{\rm hr}\left(\frac{M}{1M_\oplus}\right)^{1/2}\left(\frac{\pi_{\rm rel}}{18\mu{\rm as}}\right)^{1/2}\left(\frac{\mu_{\rm rel}}{5{\rm mas\,yr^{-1}}}\right)^{-1}. \end{aligned} \tag{1}$$

Here, $\kappa = 4G/(c^2{\rm au}) = 8.144{\rm mas}/M_\odot$ and we expect $t_{\rm E} \sim 0.05$ day assuming typical value of the lens-source relative parallax: $\pi_{\rm rel} = \pi_{\rm l}^{-1} - \pi_{\rm s}^{-1} = 1\,{\rm au}(D_{\rm l}^{-1} - D_{\rm s}^{-1}) = 18\mu$as for the bulge lens and a typical value of the lens-source proper motion in the direction of the Galactic center of $\mu_{\rm rel} = 5$ mas yr^{-1}. The lens mass M, the distance $D_{\rm l}$ to the lens and the relative proper motion $\mu_{\rm rel}$ are degenerate in the observable $t_{\rm E}$. This means that the mass function of the lens population has to be determined statistically from the $t_{\rm E}$ distribution, assuming a model of the star population density and velocities in the Galaxy. The short events in $t_{\rm E}$ distribution can be interpreted as planetary mass objects as shown in Figure 1.

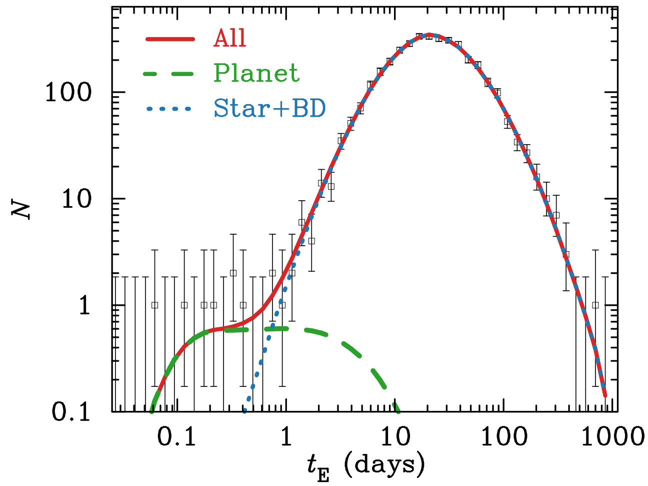

Figure 1. The observed timescale $t_{\rm E}$ distribution from the 9 year MOA-II survey (Sumi et al. 2023). The red line indicates the best fit single lens model for all population. The blue dotted line represents the known populations of stars, brown dwarfs, and stellar remnants, and the green dashed line represents the planetary mass population.

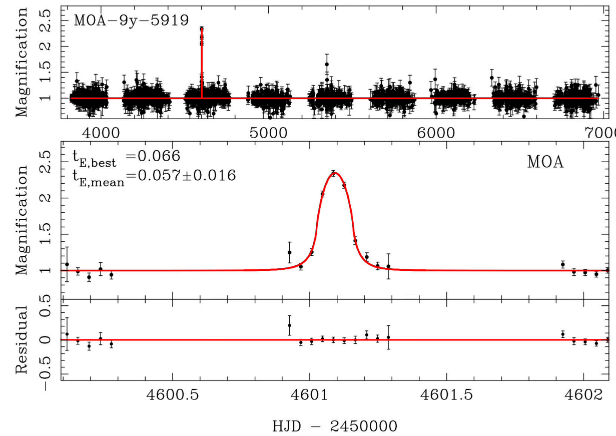

Figure 2. Light curves of the terrestrial mass microlensing candidates MOA-9y-5919 with $t_{\rm E} = 0.066$ day and $t_* = 0.092$ day.

Mróz et al. (2018) found the first short ($t_{\rm E} = 0.32$ day) event showing the Finite Source (FS) effect, i.e., a finite source and a single point lens (FSPL), in which one can measure a FS parameter $\rho = \theta_*/\theta_{\rm E}$. Here θ_* is the angler source radius which can be estimated from an empirical relation with the source magnitude and color. The $\theta_{\rm E}$ is an angular Einstein radius given by

$$\theta_{\rm E} = \frac{\mu_{\rm rel}}{t_{\rm E}} = \sqrt{\kappa M \pi_{\rm rel}}. \tag{2}$$

This value of $\theta_{\rm E}$ can give us an inferred mass of the lens with better accuracy as we can eliminate one of the three-fold degenerate terms which affecte $t_{\rm E}$, namely, $\mu_{\rm rel}$:

$$M = \frac{\theta_{\rm E}^2}{\kappa \pi_{\rm rel}} = 1 M_\oplus \left(\frac{\theta_{\rm E}}{0.7\mu{\rm as}}\right)^2 \left(\frac{\pi_{\rm rel}}{18\mu{\rm as}}\right)^{-1}. \tag{3}$$

So far, 8 short FSPL events have been discovered (Mróz et al. 2018, 2019b, 2020b,c; Kim et al. 2021; Ryu et al. 2021; Koshimoto et al. 2023). All of these have $\theta_{\rm E} < 10\,\mu$as, implying that their lenses are most likely of planetary mass.

Mróz et al. (2020b) found the short FSPL event, OGLE-2016-BLG-1928, with the smallest value of $\theta_{\rm E} = 0.842 \pm 0.064\mu$as to date. Its lens is the first terrestrial mass FFP candidate and the first evidence of such population. Koshimoto et al. (2023) found the second terrestrial mass FFP candidate MOA-9y-5919 ($t_{\rm E} = 0.057 \pm 0.016$ days, $\theta_{\rm E} = 0.90 \pm 0.14\,\mu$as) as shown in Figure 2.

For the low mass lens in the regime of $\theta_{\rm E} < \theta_*$, the timescale of magnification does not depend on $t_{\rm E}$, but it is proportional to the source angular radius as,

$$t_* = \frac{\theta_*}{\mu_{\rm rel}} = 2\,{\rm hr}\left(\frac{\theta_*}{1\mu{\rm as}}\right)\left(\frac{\mu_{\rm rel}}{5{\rm mas\,yr}^{-1}}\right)^{-1}. \tag{4}$$

So, the duration of the magnification for these terrestrial mass events is about a few hours.

Ryu et al. (2021); Gould et al. (2022) presented the $\theta_{\rm E}$ distributions from KMTNet survey. down to $\theta_{\rm E} = 4.35\,\mu$as and found a gap in the distribution of $\theta_{\rm E}$ at $9 < \theta_{\rm E}/\mu{\rm as} < 26$, which suggests a separation between the planetary mass population and other known populations, like brown dwarfs.

Recently, Sumi et al. (2023) derived the MF of the FFP by using not only $t_{\rm E}$ of the PSPL events, but also include $\theta_{\rm E}$ of FSPL events which are more informative than either $t_{\rm E}$ or $\theta_{\rm E}$ distribution alone. They determined the detection efficiency as a function of both $t_{\rm E}$ and $\theta_{\rm E}$ because finite source effects have a large influence on the detectability of microlensing events due to low-mass planets. This method is necessary for reliable results for low-mass FFPs, and it should be very useful for the analysis of Roman GBTDS which will detect many short events with FSPL.

The best fit MF of the planetary mass populations with the normalization Z relative to stars (MS+BD+WD) (integrated IMF over $3 \times 10^{-4} < M/M_\odot < 8$) can be expressed as

$$\frac{dN_4}{d\log M} = \frac{2.18^{+0.52}_{-1.40}}{{\rm dex} \times {\rm star}}\left(\frac{M}{8\,M_\oplus}\right)^{-\alpha_4}, \tag{5}$$

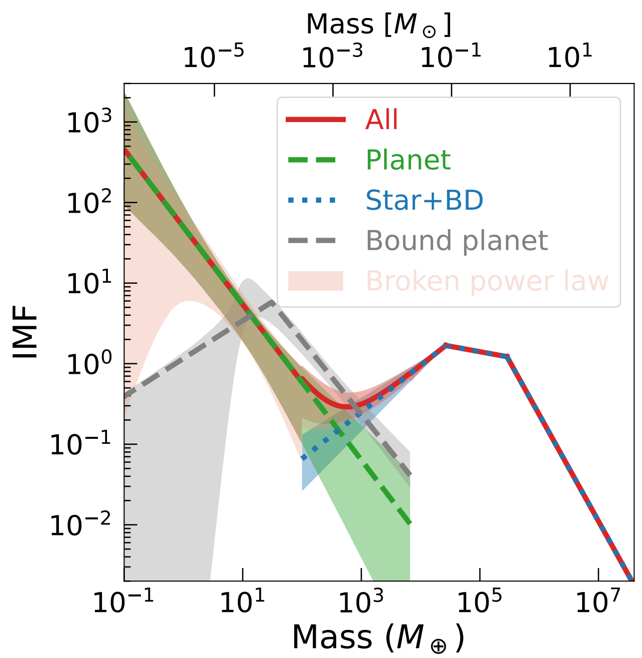

Figure 3. Initial mass function (IMF) of the best fit PL model in Sumi et al. (2023). The red line indicates the best fit for all population. The blue dotted line and green dashed line show the IMFs for the stellar and brown dwarf population and for the planetary mass population, respectively. The shaded areas indicate 1σ error. The gray dashed-line and the shaded area indicate the best-fit and 1 σ range of the bound planet MF by Suzuki et al. (2016) via microlens. The pink shaded area indicate 1σ uncertainty for the broken power law FFP model.

where $\alpha_4 = 0.96^{+0.47}_{-0.27}$. Figure 3 shows the IMF of the best fit PL model.

This implies that the number of FFPs per stars is $f = 21^{+23}_{-13}\,\mathrm{star}^{-1}$ over the mass range $10^{-6} < M/M_\odot < 0.02$.

We can measure the mass of individual FFP with $\theta_{\rm E}$ in combination with microlensing parallax $\pi_{]\rm E}$ by simultaneous ground-based or space-based observations (e.g., by Zhu, W., & Gould (2016); Bachelet & Penny (2019); Ban (2020)). This is very important to measure the mass in as many objects as possible to characterize the nature of FFP population.

2. REQUIREMENT FOR SOURCE COLOR MEASUREMENTS IN GBTDS

A precise measurement of the free floating planet mass function will require a microlensing survey that can obtain precise photometry of main sequence stars with relatively low magnification, because the small $\theta_{\rm E}$, of low-mass planetary lenses prevent high magnification. The Roman GBTDS is such a survey, and it should provide the definitive measurement of the FFP MF.

Johnson et al. (2020) predicted the $\sim$250 FFPs with masses down to that of Mars (including $\sim$30 with masses of $0.1 \le M/M_\oplus \le 1$) assuming the fiducial mass function of cold, bound planets adapted from Cassan et al. (2012). We updated the expected number of FFP events by Roman with Sumi et al. (2023)'s FM resulting $1,004^{+1878}_{-580}$ FFPs with same mass range (including 587^{+1752}_{-432} with $0.1 \le M/M_\oplus \le 1$) for single power law model and 709^{+1454}_{-430} FFPs with same mass range (including 312^{+1284}_{-278} with $0.1 \le M/M_\oplus \le 1$) for broken power law model.

The measurement of $\theta_{\rm E}$ is very informative as mentioned above. The Roman GBTDS is very sensitive to the finite source effect, i.e., ρ for low mass lenses down to $0.1 \sim 1M_\oplus$ with $\theta_{\rm E} = 0.2 \sim 0.7\mu$as because Roman observes faint dwarf sources down to $W146 < 26$ mag which have small radius $\theta_* < 0.3\mu$as.

Johnson et al. (2020) estimated that Roman GBTDS can detect the finite source effect ($\rho > 0.5$), in more than 70% and all events with lens mass of $1M_\oplus$ and $0.1M_\oplus$, respectively. However, the color measurement of the source is need to estimate $\theta_{\rm E}$. The Roman's current nominal survey plan takes observations mostly with wide F146 filter and only occasional observation with F087 and F184 alternatively every 6 hours, i.e., every 12 hours each band for the color measurements. This limits the source color measurements for short low-mass FFP events with a time scale of a few hours. So, slightly higher cadence in F087 and/or F184 should be considered for maximizing $\theta_{\rm E}$ measurements.

Johnson et al. (2020) estimated that a fraction of the events with source color measurements is only 12% and 11% with 12hr cadence of the exposures with F087 filter for $1M_\oplus$ and $0.1M_\oplus$, respectively. These can be increased to 23% and 35%, respectively, if the cadence is increased to 6 hours, and 37% and 56%, with 3 hours cadence, respectively. The increasing the cadence of F087 filter will trade with the cadence of the main F146 filter and reduce the sensitivity for detection of the shorter events. To maximize the information of FFP, it is good to balance the fraction of events with measurements of ρ and source color.

We can make a conservative assessment using Equations (12) and (13) of Penny et al. (2019) and Table B1 of Johnson et al. (2020). Assuming we delete one F146 observation every 3 or 6 hours, which would reduce the $\Delta\chi^2$ of a detection by 1/12 for every 3 hours or 1/24 for every 6 hours for relatively long events. On the other hand, for 0.1-1 $M_\oplus$, the durations of the magnification which depends on θ_* rather than $\theta_{\rm E}$, is typically $\sim$ 1.5hrs. Thus we will have $\sim$6 observations during the magnification. In events with color measurements

Table 1. Number of expected FFP events N for 12hr color cadence, a fraction of events with FS, $f_{\rm FS}$, a fraction of color measurement, $f_{\rm color}$, a ratio of expected FFP events with 3hr color cadence relative to N, and the number of filter changes per survey, $N_{\rm filter}$ for each color's cadence.

Mass	N	$f_{\rm FS}$		$f_{\rm color}$		$N_{\rm 3hr}/N$
	(12hr)	(12hr)	(12hr)	(6hr)	(3hr)	(3hr)
$0.1M_\oplus$	187^{+2344}_{-187}	100%	11%	35%	56%	95%
$1M_\oplus$	273^{+455}_{-222}	70%	12%	23%	37%	97%
$N_{\rm filter}$	–	–	$1,728$	$3,456$	$6,912$	–

given above, one of 6 F146 observations is deleted due to a color measurement. In this case, $\Delta\chi^2$ would be reduced by 1/6, so the ratio of $\Delta\chi^2$ given by Eq. (12) of Penny et al. (2019) become $\delta = \Delta\chi^2_{\rm new}/\Delta\chi^2_{\rm old} = (1-1/6)/1 = 5/6$. From the table B1of Johnson et al. (2020), $\alpha = 0.19$ and 0.28 for 1 $M_\oplus$ and 0.1 $M_\oplus$, respectively. From Eq. (13) of Penny et al. (2019), the new yield of Earth mass planets would be $\delta^\alpha = 0.97$ and 0.95 times the yield with color filter observation every 12 hours for 1 $M_\oplus$ and 0.1 $M_\oplus$, respectively. This is conservative, because the events without color measurement does not have any effect and the color filter observations will also contribute to $\Delta\chi^2$, and limit the negative impact of having gaps in the W146 time-series. These numbers are summarized in Table 1.

The impacts for reducing the main F146 filter is limited, compared to the gain by increasing the color filter and thus the higher cadence of around 3 hours is preferred.

The other potential cost to the mission is the number of filter wheel movement which may impact the mission lifetime. The survey with a color observation every 12 hours requires 4 filter wheel movements per day, which is $4 \times 72 \times 6 = 1,728$ activations per survey. One color observation every 3 hours would require 6,912 changes. These numbers are summarized in Table 1.

In addition to the $\theta_{\rm E}$ measurements, color measurement is important to eliminate the false positives. The main source of the false positives of short FFP event is flare stars. The color during the flare is bluer than the source which result irregular position on the CMD. This is qualitatively important for selecting the clean sample of FFP.

Mróz et al. (2020c) and Johnson et al. (2020) also pointed out that the color measurement is useful to break the degeneracy between the source flux $f_{\rm s}$ and ρ for the case of large ρ in which the magnification is almost constant not depending on u_0. The source color helps to estimate $f_{\rm s}$, then to get a precise ρ.

The more color observations would have a positive impact on transiting planet science that can be done with the GBTDS, i.e., better false positive rejection (Montet, Yee & Penny 2017; Wilson, Barclay & Powell 2023).

REFERENCES

Bachelet, E., & Penny, M. 2019, ApJL880, L32

Ban, M. 2020, MNRAS, 494, 3235

Cassan, A., Kubas, D., Beaulieu, J. P., et al. 2012, Nature, 481, 167, doi: 10.1038/nature10684

Gould, A. et al. 2022, Journal of the Korean Astronomical Society, 55, 173

Johnson, S. A., Penny, M. & Gaudi, B. S., et al. 2020, AJ, 160, 123

Kim, H.-W., Hwang, K.-H., Gould, A., et al. 2021, AJ, 162, 15

Koshimoto, N., Baba, J., & Bennett, D. P. 2021a, ApJ, 917, 78. doi:10.3847/1538-4357/ac07a8

Koshimoto, N., Sumi, T. and Bennett, D. P., et al. 2023, AJ. in press, arXiv:2303.08279 (K23)

Lin, D. N. C. & Ida, S. 1997, ApJ, 477, 781. doi:10.1086/303738

Montet, B. T., Yee, J. C., & Penny, M. T. 2017,PASP, 129, 044401

Mróz, P. Udalski A., Skowron, J., et al. 2017, Nature, 548, 183

Mróz, P. Y.-H.Ryu, Skowron, J., et al. 2018, ApJ, 155, 121

Mróz, P. Udalski A., Skowron, J., et al. 2019, ApJS, 244, 29

Mróz, P. Udalski A., Bennett, D. P. et al. 2019, å, 622, A201

Mróz, P. Udalski A., Szymański, M., et al. 2020, ApJS, 249, 16

Mróz, P., Poleski, R. & Gould, A. 2020, ApJ, 903, 11

Mróz, P., Poleski, R., Han, C. 2020, AJ, 159, 262

Paczyński, B. 1991, ApJ, 371, L63

Penny, M. T., Gaudi, B. S., Kerins, E., et al. 2019, ApJS, 241, 3

Rasio, F. A. & Ford, E. B. 1996, Science, 274, 954. doi:10.1126/science.274.5289.954

Ryu, Y-H, Mróz, P., Gould, A. 2021, AJ, 161, 126

Sumi, T. et al., 2011, Nature, 473, 349

Sumi, T., Koshimoto, N., & Bennett, D. P. et al., 2023, AJ, submitted,arXiv:2303.08280

Suzuki, D. Bennett, D. P. & Sumi T. et al., 2016, ApJ, 833, 145

Weidenschilling, S. J. & Marzari, F. 1996, Nature, 384, 619. doi:10.1038/384619a0

Wilson, R. F., Barclay, T., & Powell, B. P. . 2023, arXiv:2305.16204

Zhu, W., & Gould, A. 2016, JKAS, 49, 93